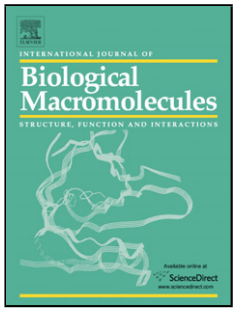

Title: Novel Inhibitors of Tyrosinase Produced by the 4-substitution of TCT (Π)

Authors: Jing Liu, Mengrong Li, Yanying Yu, Shuwen Cao

PII: S0141-8130(17)30163-0
DOI: http://dx.doi.org/doi:10.1016/j.ijbiomac.2017.05.036
Reference: BIOMAC 7525

To appear in: *International Journal of Biological Macromolecules*

Received date: 11-1-2017
Revised date: 2-5-2017
Accepted date: 8-5-2017

Please cite this article as: Jing Liu, Mengrong Li, Yanying Yu, Shuwen Cao, Novel Inhibitors of Tyrosinase Produced by the 4-substitution of TCT (Π), International Journal of Biological Macromoleculeshttp://dx.doi.org/10.1016/j.ijbiomac.2017.05.036

Research highlights

1. Intermolecular interactions between inhibitor and amino acid residues ASN81 of enzyme

2. The 4-benzoy methoxy substitution of TCT produced new novel tyrosinase inhibitors

3. The inhibitor introduced secondary and tertiary conformational changes in enzyme

Novel Inhibitors of Tyrosinase Produced by the 4-substitution of TCT (II)

Jing Liu[a], Mengrong Li[a], Yanying Yu [a], Shuwen Cao [a,b]*

[a]*Department of Chemistry, Nanchang University, Nanchang 330031, PR China*

[b]*State Key Laboratory of Food Science and Technology, Nanchang University, Nanchang 330047, PR China*

[*]*Corresponding author. Tel.: +86 0791 83969610. Fax: +86 0791 83969610.*

E-mail address: caosw@ncu.edu.cn (S.-W.Cao).

Abstract

Novel Tyrosinase Inhibitors of 4-functionalized Thiophene-2-carbaldehyde thiosemicarbazone (TCT) derivatives (**1**-**8**) had been synthesized and Spectrofluorimetry, ^{1}H and ^{13}C NMR titration and Molecular docking had been used to investigate their inhibitory activities and mechanisms on tyrosinase. The results showed that the inter-molecular interactions or hydrogen bond formation by increasing length of carbon chain or introducing benzene ring to the 4-functionalized ester group promoted or stabilized formation of complexes between modifier and tyrosinase, and enhanced the inhibitory activity of modifiers. The inhibitory activity of 4-benzoy methoxy-TCT was much stronger than that of any other synthesized tested modifiers, which was well explained by molecular docking and further verified by spectrofluorimetry and NMR titration by assuming that there existed an inter-molecular interaction besides formation of hydrogen bonds between the amino

acid residues ASN260, GLU256, HIS85 of enzyme and the modifier.We concluded that 4-benzoy methoxy substitution of TCT was a good route obtaining novel tyrosinase inhibitors and deserved further studies.

Keywords: Thiophene-2-carbaldehyde thiosemicarbazone (TCT) derivatives; Tyrosinase inhibitors; Spectrofluorimetry; ^{1}H and ^{13}C NMR titration.

1. Introduction

Tyrosinase (EC 1.14.18.1), a kind of metalloenzyme with dinuclear copper ions, is common in animals, insects and microorganisms [1]. Tyrosinase belongs to the Type-3 copper protein family, there are two closely spaced copper ions at the active site of the structures, each of them is coordinated by three His residues through nitrogen atoms [2]. Generally, tyrosinase can catalyze the rate-limiting step in the biosynthetic pathway of melanin pigments, is widely distributed in nature [3]. The enzyme participates in several important reactions of host defence, wound healing and sclerotization in insects and other arthropods [4]. Tyrosinase has also been found to be responsible for undesired enzymatic browning of farm products, such as bruised or cut fruits and vegetables, which subsequently leads to a significant decrease in their nutritional and market values[5]. Moreover, pigmentation, melanoma and Parkinson's syndrome are also closely related to it [6, 7].

To find naturally occurring or synthesize novel tyrosinase inhibitors is receiving a considerable attention from scientists of food, medicine, chemistry and animal fields [8-12]. As an outcome of these studies, a huge library of tyrosinase inhibitors has been discovered from natural sources or synthesized in the laboratories. However, these inhibitors such as kojic acid, arbutin, etc, have been troubled by the cost, effectiveness, safety [13]. Although in our prior study of some novel tyrosinase inhibitors, TCT and its modifier of 4-methoxyacetyl -TCT, we obtained a preliminary understanding of the structure-activity relationships and inhibitory mechanisms between these modifiers and target enzymes by using fluorescence, ^{1}H NMR titration and molecular docking

studies [14,15]. However, we still have little understanding of how the structure-activity relationships and inhibitory mechanisms affect the inhibitory activities when modifying TCT by increasing length of carbon chain or introducing ring of cyclocarbon or benzene to the 4-functionalized ester group aiming at changing chemical micro-environment of hydrophobic domain of tyrosinase active center. Generally, this type of structural modifications either increases or decreases the inhibitory activity of the modifier. Based on our understanding of the structure-activity relationship of 4-methoxyacetyl -TCT, we find it possible to increase the inhibitory activity of a modifier by introducing an appropriate functional group at the thiophene ring on TCT, assuming that the introduced group promotes the formation of complexes between the sulfur atom from the thiourea of target modifiers and the copper ion of the enzyme active center. It is necessary to find new novel tyrosinase inhibitors with strong inhibitory activities to better our understanding of the structure-activity relationship of TCT.

With the advancement of science and technology, it is clear that good inhibitory activity, bearable and acceptable toxicity were fundamental requirements for a compound taken as a reasonable precursor undertaken chemical modifying aimed at finding potential novel tyrosinase inhibitors. Based on this standard, we had investigated the related toxicity data of TCT and found that it was a reasonable and appropriate precursor (https://chem.sis.nlm.nih.gov) for finding candidates for potential tyrosinase inhibitors of food additives [15].

Novel Tyrosinase Inhibitors of 4-functionalized TCT derivatives (**1-8**) were

designed, synthesized and evaluated for their inhibitory and mechanisms on tyrosinase by using Spectrofluorimetry, ^{1}H and ^{13}C NMR titration and Molecular docking. Our study helped further clarify the relationship between modifiers and tyrosinase and understand effects on inhibitory activity introduced by modifying TCT with increasing length of carbon chain or introducing ring of cyclocarbon or benzene to the 4-functionalized ester group of TCT, which may provide a promising route to obtain novel and highly potent tyrosinase inhibitors.

2. Materials and methods

2.1. Chemicals and reagents

Mushroom tyrosinase (EC 1.14.18.1) and L-3, 4-dihydroxyphenyl-alanine (L-DOPA) were purchased from Sigma (St. Louis, MO, USA). 2-thiophenecarboxaldehyde and thiosemicarbazide were obtained from J&K Chemical Co (Shanghai, China). All other reagents were local and of analytical grade. The water used was re-distilled and ion-free.

2.2. Synthesis

The method of synthesis of intermediates and target compounds is described in Fig.1, as references with yield improvement of reactions of 4-chloromethyl- and 4-hydroxymethyl to 65% and 70% [16-19], respectively.

For the synthesis of all intermediates of acid chlorides described in Fig. 1, (B), the strict control of the reaction conditions (n acid:n$SOCl_2$=1.25:1) was needed. When the reaction of synthesizing acid chloride was completed, the produced liquid was

dropped directly into the cold mixture of 4-hydroxymethyl-2-thiophene formaldehyde with dichloromethane, and then the intermediate of Acylmethoxy-2-thiophene carboxaldehyde was received. Finally, the target compounds 1-8 were produced by the reaction depicted in Fig. 1, (B) with the yield of about 90% [20].

ESI–MS data were obtained on a Agilent 6545 Q-TOF LC/MS (USA), and NMR data were acquired on a 400 MHz NMR spectrometer (DD2-400) from Agilent (USA).The IR spectra were measured with KBr pellets on a Nicolet 5700 FT-IR spectrometer(USA).

4-Formyl methoxy-2-Thiophenealdehyde thiosemicarbazone (**1)**: yellow crystals, yield 23.4%, IR (KBr) 3155.34, 1721.70, 1598.55, 1528.20. ^{1}H NMR (400 MHz, DMSO-d_6) δ 11.43 (s, 1H, NH), 8.28 (s, 1H, -CO-H), 8.21 (s, 1H, NH-H), 8.18 (s, 1H, NH-H), 7.62 (s, 1H, thiophene-H), 7.57 (s, 1H, CH), 7.41 (s, 1H, thiophene-H), 5.09 (s, 2H, CH_2). ^{13}C NMR (100 MHz, DMSO-d_6) δ177.99 (1C, C=S), 162.34 (1C, C= O), 139.68 (1C, C= N), 137.63 (1C, 2-thiophene), 137.47 (1C, 4 -thiophene), 131.03 (1C, 3-thiophene), 128.00 (1C, 5-thiophene), 60.43 (1C, CH_2). MS (ESI): m/z 244.0208$[M+H]^+$.

4-Acetyl methoxy-2-Thiophenealdehyde thiosemicarbazone(**2**) [15]: synthesized as the contrast.

4-Propionyl methoxy-2-Thiophenealdehyde thiosemicarbazone(**3**): yellow crystals, yield 33.6%, IR(KBr) 3154.38, 1729.59, 1596.17, 1534.91.^{1}H NMR (400 MHz,

DMSO-d_6) δ 11.44 (s, 1H, NH), 8.21, 8.17 (d, 2H, NH_2), 7.58 (s, 2H, thiophene-H, CH), 7.39 (s, 1H, thiophene-H), 5.00 (s, 2H, CH_2), 2.34 (q, J = 7.5 Hz, 2H, CH_2), 1.01 (t, J = 7.5 Hz, 3H, CH_3). ^{13}C NMR (100 MHz, DMSO-d_6) δ177.99 (1C, C=S), 173.90(1C, C=O), 139.58 (1C, C=N), 138.07(1C, 2-thiophene), 137.69(1C, 4-thiophene), 131.01(1C, 3-thiophene), 127.55(1C, 5-thiophene), 61.00(1C, CH_2). MS (ESI): m/z 272.0520$[M+H]^+$.

4-Butyryl methoxy-2-Thiophenealdehyde thiosemicarbazone(**4**): brown crystals, yield 32.7%, IR(KBr) 3153.14，1730.54, 1599.75, 1530.33. ^{1}H NMR (400 MHz, DMSO-d_6) δ 11.42 (s, 1H, NH), 8.19 (s, 1H, NH_2), 8.17 (s, 1H, NH_2), 7.57 (s, 1H, thiophene-H), 7.55 (s, 1H, CH), 7.38 (s, 1H, thiophene-H), 5.00 (s, 2H, CH_2), 2.29 (t, J=7.2 Hz, 2H, CH_2), 1.53 (dd, J = 14.7, 7.3 Hz, 2H, CH_2), 0.85 (t, J = 7.4 Hz, 3H, CH_3). ^{13}C NMR (100 MHz, DMSO-d_6) δ 178.01(1C, C=S),173.05 (1C, C=O), 139.59(1C, C=N), 138.07(1C, 2-thiophene), 137.70(1C,4-thiophene), 131.02(1C, 3-thiophene), 127.60 (1C, 5-thiophene), 60.93(1C, CH_2), 35.69(1C, CH_2), 18.36(1C, CH_2), 13.86(1C, CH_3). MS (ESI): m/z 286.0677$[M+H]^+$.

4-Pentanoyl methoxy-2-Thiophenealdehyde thiosemicarbazone (**5**) yellow crystals, yield 33.2%, IR (KBr) 3153.13, 1733.73, 1599.75, 1529.78. ^{1}H NMR (400 MHz, DMSO-d_6) δ 11.42 (s, 1H, NH), 8.19 (s, 1H, NH_2), 8.17 (s, 1H, NH_2), 7.57 (s, 1H, thiophene-H), 7.56–7.50 (m, 1H, thiophene-H, CH), 7.38 (s, 1H, thiophene-H), 5.03 (d, J = 23.2 Hz, 2H, CH_2), 2.31 (t, J = 7.4 Hz, 2H, CH_2), 1.57 – 1.42 (m, 2H, CH_2),

1.33 – 1.18 (m, 2H, CH_2), 0.83 (t, J = 7.3 Hz, 3H, CH_3) ^{13}C NMR (100 MHz, DMSO-d_6) 178.00(1C, C= S), 173.18(1C, C=O), 139.57(1C, C=N), 138.06(1C, 2-thiophene), 137.68(1C, 4-thiophene), 131.01(1C, 3-thiophene), 127.58 (1C, 5-thiophene), 60.94(1C, CH_2), 33.55(1C, CH_2), 26.96(1C, CH_2), 22.03(1C, CH_2), 14.04(1C, CH_2). MS (ESI): m/z 300.0833$[M+H]^+$.

4-Cyclopentanecarbonyl methoxy-2-Thiophenealdehyde thiosemicarbazone(**6**): yellow crystals, yield 34.8%, IR(KBr) 3152.59, 1728.83, 1598.85, 1529.80.^{1}H NMR (400 MHz, DMSO-d_6) δ 11.42 (s, 1H, NH), 8.20 (s, 1H, NH_2), 8.17 (s, 1H, NH_2), 7.56 (s, 2H, thiophene-H, CH), 7.38 (s, 1H, thiophene-H), 5.00 (s, 2H, CH_2), 2.76 (p, J = 7.8 Hz, 1H, CH), 1.80 (s, 2H, CH-H), 1.66 (dd, J = 16.2, 10.8 Hz, 2H, CH-H), 1.61 – 1.43 (m, 4H, CH_2, CH_2). ^{13}C NMR (100 MHz, DMSO-d_6) δ178.02(1C, C=S), 175.95(1C, C=O), 139.61(1C, C=N), 138.15(1C, 2-thiophene), 137.70 (1C, 4-thiophene), 130.94(1C, 3-thiophene), 127.48(1C, 5-thiophene), 61.10(1C, CH_2), 43.37(1C, CH_2), 29.90(2C, CH_2), 25.80(2C, CH_2). MS (ESI): m/z 312.0833$[M+H]^+$.

4-Cyclohexaformyl methoxy-2-Thiophenealdehyde thiosemicarbazone(**7**): yellow crystals, yield 34.0%, IR(KBr) 3155.40, 1726.98, 1598.87, 1530.58.^{1}H NMR (400 MHz, DMSO-d_6) δ 11.43 (s, 1H, NH), 8.20 (s, 1H, NH-H), 8.17 (s, 1H, NH-H), 7.56 (s, 2H, thiophene-H, CH), 7.38 (s, 1H, thiophene-H), 4.99 (s, 2H, CH_2), 2.32 (t, J = 10.8 Hz, 1H, CH), 1.80 (d, J = 12.1 Hz, 2H, CH-H), 1.63 (d, J = 12.3 Hz, 2H, CH-H), 1.55 (d, J = 11.2 Hz, 1H, CH-H), 1.39–1.11 (m, 6H, Cyclohexane-H). ^{13}C NMR (100

MHz, DMSO-d_6) δ 178.00(1C, C=S), 175.17(1C, C=O), 139.60(1C, C=N), 138.13(1C, 2-thiophene), 137.70(1C, 4-thiophene), 130.86(1C, 3-thiophene), 127.34 (1C, 5-thiophene), 60.98(1C, CH_2), 42.51(1C, CH_2), 28.98(2C, CH_2), 25.71(1C, CH_2), 25.20(2C, CH_2). MS (ESI): m/z 326.0991$[M+H]^+$.

4-Benzoy methoxy-2-Thiophenealdehyde thiosemicarbazone (**8**): yellow crystals, yield 35.6%, IR (KBr) 3153.18, 1714.51, 1598.58, 1526.30. ^{1}H NMR (400 MHz, DMSO-d_6) δ 11.44 (s, 1H, NH), 8.19 (s, 2H, NH_2), 7.99 (s, 1H, thiophene-H), 7.97 (d, J = 1.3 Hz, 1H, CH), 7.70 (s, 1H, thiophene-H), 7.65 (t, J = 7.4 Hz, 1H, benzene-H), 7.57 (s, 1H, benzene-H), 7.55 – 7.47 (m, 3H, benzene-H), 5.27 (s, 2H, CH_2). ^{13}C NMR (100 MHz, DMSO-d_6) δ 178.01(1C, C=S), 165.98(1C, C=O), 139.75(1C, C=N), 137.83(1C, 2-thiophene), 137.71(1C,4-thiophene), 133.95(1C, benzene), 131.05(1C, 3-thiophene), 129.92(1C, benzene), 129.73(2C, benzene), 129.27(2C, benzene), 127.83(1C, 5-thiophene), 61.97(1C, CH_2). MS (ESI): m/z 320.0518$[M+H]^+$.

2.3. Enzyme activity assay

The assay of inhibition of target compounds on the diphenolase activity of mushroom tyrosinase was performed by our reported procedure with minor modifications [14]. L-DOPA was used as substrate for the enzyme activity assay. The reaction media (3 mL) for activity assay contained 2.8 mL 0.5 mM L-DOPA in 50 mM Na_2HPO_4-NaH_2PO_4 buffer (pH 6.8) and 0.1 mL of different concentrations of inhibitor (dissolved in DMSO previously). 0.1 mL of the aqueous solution of

mushroom tyrosinase was added to the mixture. The solution was immediately monitored by measuring the linear increase in optical density at 475 nm of formation of the DOPA chrome for 150s using a Shimadzu UV-2450 spectrophotometer (Japan). The extent of inhibition by the addition of the sample was expressed as the percentage necessary for 50% inhibition (IC_{50}), calculated by SPSS19. The value of relative enzymatic activity can be calculated by the following equation:

$$\text{Relative enzymatic activity (\%)} = \triangle OD_1 / {}^{\triangle}OD_2 \times 100\%$$

Where $\triangle OD_1$ and $\triangle OD_2$ are the enzyme activity value of the reaction system with inhibitor and reagent blank,respectively. Kojic acid was used as reference standard inhibitors for comparison.

2.4. Determination of the inhibition mechanism and the inhibition type

Determination of inhibition mechanism was assayed by maintaining the concentration of L-DOPA (0.5 mM) and changing the concentration of the enzyme (16, 12, 8, 4 μg /mL) in reaction medium. The enzyme activity was measured for different concentrations of inhibitor. Determination of inhibition type and inhibition constants was assayed by maintaining the concentration of enzyme (10 μg/mL) and changing the concentration of the L-DOPA (0.5, 1, 1.5, 2 mM) in reaction medium [15]. The inhibition type was assayed by the Lineweaver–Burk plot, and inhibition constants (K_I or K_{IS}) were determined by the second plots of the apparent K_s/V_m or $1/V_m$ versus the concentration of inhibitor [21], the equation can be written as:

$$\frac{1}{V} = \frac{K_S}{V_m[S]}\left(1 + \frac{[I]}{K_I}\right) + \frac{1}{V_m}\left(1 + \frac{[I]}{K_{IS}}\right)$$

The V is the reaction velocity; K_S is the Substrate constant; Vm is the maximal

velocity; [*I*] is the concentration of inhibitor; [*S*] is the concentration of substrate; K_I is the constants for the inhibitor binding with the free enzyme and K_{IS} is the constants for the inhibitor binding with enzyme substrate complex, They were obtained from the slope or the vertical intercept versus the inhibitor concentration, respectively.

2.5. Fluorescence assay

The fluorescence quenching experiment was performed with reference [22]. The reaction media (2 mL) contained 1.8 mL Na_2HPO_4-NaH_2PO_4 buffer (pH = 6.8, 50mM) and 0.2 mL of the aqueous solution of mushroom tyrosinase(30 μg/mL), and then titrated by successive addition of compounds **1**, **6**, **8** and **6**-Cu^{2+} complex (the constituent ratio of ligand and Cu^{2+} was 2:1, the chelation ratio has been determined by continuous variation method) [23] ,solution using a pipette (the concentrations ranging from 0 to 94.12 μM, while the concentrations of compound **8** just half of it). Fluorescence intensities were recorded using a Hitachi F-4600 spectrofluorophotometer (Japan) at three different temperatures (30, 35 and 40 ^{0}C) with an excitation wavelength of 280 nm, while excitation and emission slit widths are 10 nm and 5 nm respectively.

To eliminate the probability of re-absorption and inner filter effects in UV absorption, all of the fluorescence data were corrected for absorption of exciting light and emitted light on the basis of the following relationship [24]:

$$F_{corr} = F_{obs} e^{(A_1+A_2)/2}$$

F_{corr} and F_{obs} are the corrected and observed fluorescence intensities, respectively. A_1 and A_2 are the absorbances of inhibitor at the excitation and emission wavelengths, respectively. Fluorescence quenching was described by the well-known Stern-Volmer

equation:

$$\frac{F_0}{F} = 1 + K_q\tau_0[Q] = 1 + K_{sv}[Q]$$

Where F_0 and F are the fluorescence intensities before and after the addition of the quencher, respectively, K_q is the bimolecular quenching constant, τ_0 (10^{-8} s) is the lifetime of the fluorophore in the absence of the quencher, [Q] is the concentration of the quencher, and K_{SV} is the Stern–Volmer quenching constant.

For the static quenching interaction, if it is assumed that there are similar and independent sites in the biomolecule, the apparent binding constant (K_a) and the number of binding sites (n) can be calculated by the following equation [25]:

$$\log\frac{F_0 - F}{F} = logK_a + nlog[Q]$$

Synchronous fluorescence spectra were recorded by setting the excitation and emission wavelength interval (Δλ) at 15 and 60 nm over a wavelength range of 270-320 nm and 250-320 nm, respectively [26].

The three-dimensional fluorescence spectra were measured under the following conditions: the emission wavelength was recorded between 200 and 450 nm, and the initial excitation wavelength was set at 200 nm with an increment of 5 nm.

2.6. ^{1}H NMR and ^{13}C NMR titration

^{1}H NMR titration studies were performed to investigate the interaction between the compounds **1**, **6**, **8** and tyrosinase. A 0.5 mL of 21 mM solution of compounds **1**, **6**, **8** in DMSO-d6 was prepared and titrated with tyrosinase solution by using a micropipette (to final concentrations ranging from 0, 0.098 to 0.341 mg/mL). While ^{13}C NMR titration of compound **8** (62.6 mM) in DMSO-d6 was prepared and titrated

with tyrosinase solution from 0 to 0.406 mg/mL. After each addition of tyrosinase, the ^{1}H NMR and ^{13}C NMR spectra were recorded and the changes in the chemical shift of the protons were noted.

2.7. Molecular docking study

Molecular docking is an application wherein molecular modeling techniques are used to predict how a protein (enzyme) interacts with small molecules (ligands) [27-29]. The active site was docked with inhibitors using the dock suite of Accelrys Discovery Studio 2.0 software (Accelrys, Inc.). The 3D structure of compound **8** was generated in Chem3D Ultra 8.0, and the X-ray crystal structure of Agaricus bisporus tyrosinase (PDB ID: 2Y9W) was retrieved from the RCSB Protein Data Bank (http://www.rcsb.org/pdb). All crystallographic water molecules, solvent molecules and ions were removed from the protein structure. The forcefield CHARMm function was used to roughly search the conformations when compounds docked into tyrosinase, and then the modified tyrosinase was selected as the binding site for the study and expanded to make the cavity. Subsequently, the conformations of compounds were optimized using the same forcefield function, followed by flexibly being docked in a stepwise manner with the protocol of Dock ligands. The docked conformation, which had the highest score, was selected to analyze the mode of binding. The outputs were further rendered with Pymol to obtain visible combination models.

3. Results and discussion

3.1. Effect and inhibition mechanism of thiosemicarbazone derivatives on the

diphenolase activity of mushroom tyrosinase

The IC_{50} values of the compounds **1**-**8** were listed in Table 1, Kojic acid, TCT and 4-acetyl methoxy-TCT (compound **2**) was used as comparative reference standard inhibitors. In previous work we found that TCT (thiophene 2-carboxaldehyde thiosemicarbazone) have stronger inhibitory effect for tyrosinase (IC_{50} =0.43 μM), this is mainly attributed to an auxiliary vicinity synergistic effect of the thiophene ring [14]. Further research revealed that it was beneficial to the improvement of the activity that the 4- position of thiophene rings was substituted by acetylmethoxy group (IC_{50} = 0.34 μM). We assumed that this favorable effect may root from the much stronger auxiliary vicinity synergistic effect from the 4- acetylmethoxy substitution group of TCT than that from TCT itself. In order to better understand effects on inhibitory activity introduced by modifying TCT with increasing length of carbon chain or introducing ring of cyclocarbon or benzene to the 4-functionalized ester group of TCT, we synthesized a series of new 4-functionalized TCT derivatives (**1**-**8**).

As shown in Table 1 we can found that the inhibition activity of modifier was well enhanced as the increasing of length of the alkyl carbon chain or introducing cyclocarbon ring to the 4-functionalized ester group of thiophene ring of TCT. Interestingly, the improvement of inhibitory activity of modifier was greatly enhanced by introducing benzene ring to the same position as cyclocarbon ring of TCT (IC_{50} =0.068 μM), in which the inhibitory activity was increased 68.52% compared to that of 4-acetyl methoxy-TCT (compound **2**). The reasonable explanation for the

enhancement from the chemical modification by increasing length of substituted group was that when the length of the alkyl carbon chain was increased or the cyclocarbon ring was introduced to the 4-functionalized ester group of thiophene ring of TCT, the formation of complexes between the inhibitor and tyrosinase was promoted and enhanced due to improvement inter-molecular interaction between the inhibitor and hydrophobic domain located in the active center of enzyme. The great increase of inhibitory activity from the chemical modification by introducing benzene ring to the 4-functionalized ester group of thiophene ring of TCT may partially attribute to the much stronger inter-molecular interaction i. e. Vander Waals Force [30] between introducing benzene ring and hydrophobic domain of enzyme active center, which either increases the inhibitory activity of the modifier by disrupting both tertiary and secondary structures of the tyrosinase or greatly promotes the formation of complexes between the inhibitor and tyrosinase. These explanations were verified by followed experiment data of spectrofluorimetry studies and well consistent with the results of molecular docking depicted in Fig. 6.

Subsequently, the inhibitory mechanism of compounds **1-8** against tyrosinase for the oxidation of L-DOPA had been studied. Fig.2A showed that the plots of the enzymatic activity versus the concentrations of enzyme in the presence of different concentrations of the inhibitors gave a family of straight lines that all passed through the origin. A linear slope decrease with increasing concentration of the inhibitors indicated that the inhibition caused by the inhibitors on tyrosinase was reversible [31, 32]. The inhibition type of inhibitors on tyrosinase was assayed using the

Lineweaver-Burk plots of the reciprocal of the reaction rate versus the reciprocal of the substrate concentration. As shown in Fig. 2C, the double-reciprocal plots yielded a group of straight lines intersecting at the second quadrant, which indicated that these inhibitors most probably belonged to mixed-type inhibitors [21].

3.2 Spectrofluorimetry studies

3.2.1. Synchronous fluorescence

Synchronous fluorescence spectroscopy can provide information about the micro-environmental alterations around fluorophores (tyrosine and tryptophan) of tyrosinase, and understanding of conformation changes of enzyme.

As shown in Fig. 3 (A) and Fig. 3(B), the maximum emission wavelength of tyrosine residues had a slight blue shift from 293.8→290.0 nm, while wavelength of tryptophan residues had a slight red shift from 280.2→284.0 nm, which suggested that the hydrophobicity and polarity around tyrosine and tryptophan residues of tyrosinase were increased due to enhanced inter-molecular interaction (Van der Waals force) between inhibitor and tyrosinase [26].

3.2.2. Three-dimensional fluorescence

The three-dimensional fluorescence spectroscopy has been recently employed as a novel probe to monitor the secondary and tertiary conformation changes in proteins [33]. As is well known, the peaks **1**(λ_{ex} = 225 nm, λ_{em} = 345 nm) and peak **2** (λ_{ex} = 280 nm, λ_{em} = 360 nm) represented typical fluorescence peaks of protein. The peak **2** was related to the fluorescence spectral characteristics of Trp and Tyr residues due to $\pi \rightarrow \pi^*$ transition, showing changes in the tertiary structure [34], whereas peak **1**

represented the fluorescence characteristics of the polypeptide backbone as a result of n→π* transition, a probe for secondary structural changes [35].

Three-dimensional (3D) fluorescence spectra of tyrosinase in absence and presence of compounds **1, 6** and **8** were performed. As shown in Fig. 3(a-d), we observed different decreases of the fluorescence intensity of peak **1** and peak **2** for tyrosinase under the same concentration of compounds **1, 6** and **8**. Among them, the largest decrease of the fluorescence intensity is tyrosinase in presence of compound **8** with decrease of 90.78% for peak **1** and 60.29% for peak **2**, which indirectly suggested that the interaction (Van der Waals force) between tyrosine and tryptophan residues of tyrosinase and benzene ring moiety of compound **8** was the most powerful. The decrease of the fluorescence intensity for the two peaks suggested that unfolding of the polypeptide chain leads to the conformation changes and increases the exposure of some buried sites (Trp/Tyr/peptide groups). These results suggested that the disruption of both tertiary and secondary structures of the tyrosinase in inhibitor-complex state [36] helped to enhance the inhibitory activity of inhibitor.

The calculations characteristic 3D parameters of other compounds are reported in Table 2.

3.2.3. Fluorescence quenching of tyrosinase by inhibitors

The above studies suggested that the interaction between enzyme and inhibitors may lead to change the surrounding chemical micro-environment of the active site of tyrosinase. Therefore, in order to further understand reaction mechanism between enzyme and inhibitors, we exploited fluorescence spectroscopy to characterize the

binding between small molecule and enzyme. The fluorescence emission spectra of tyrosinase in the absence or in the presence of compound **6** excited at 280 nm are shown in Fig. 4(A). Obviously, the enzyme displayed a strong emission peak at 367.4 nm, which resulted from the tryptophan and tyrosine residues of tyrosinase [37]. With increasing the amounts of compound **6**, the fluorescence emission peak of enzyme decreased significantly and regularly with a latter shift of the emission peak's position, which indicated that inhibitors interacted with tyrosinase and quenched the intrinsic fluorescence of enzyme. The plots of F_0-F/F versus [Q] at three different temperatures (303, 308, and 313 K) are shown in Fig. 4(A) inset, and the corresponding K_{SV} values for the complexation of small molecule with tyrosinase are given in Table 1. A high linearity suggested that only one type of quenching process occurred, either static or dynamic quenching [38]. The K_{SV} values clearly displayed a decreasing tendency with increasing temperature, and the calculated K_q values at 303, 308, and 313 K were 1.318×10^{12}, 1.299×10^{12} and 1.113×10^{12} $L\cdot mol^{-1}\cdot s^{-1}$, respectively, which were considerably greater than the maximum scatter collision quenching constant of various quenchers with biopolymers, 2.0×10^{10} $L\cdot mol^{-1}\cdot s^{-1}$[39], which indicates that the mechanism of the fluorescence quenching of tyrosinase was static and resulted from the formation of a inhibitors-enzyme complex.

To further investigate the acting site between the inhibitor and enzyme, we performed a fluorescence titration of tyrosinase with **6**-Cu^{2+} complex. As illustrated in Fig. 4(B), the increased concentration of the **6**-Cu^{2+} complex led to a similar decrease in the intensity of the emission band at 367.2 nm like compound **6**, However, because

of the overlap between the tyrosinase fluorescence and the **6**-Cu^{2+} complex absorbance, the decreased intensity was likely related to the quenching by the fluorescence resonance energy transfer (FRET) [40]. The static quenching binding constant (*Ka*) of the **6**-Cu^{2+} complex was $10^{2.255}$ L•mol^{-1}•s^{-1} at 30^0C, less than the static quenching of the binding constant (*Ka*) of compound **6** ($10^{4.022}$ L•mol^{-1}•s^{-1}). The results showed that the copper ion may have occupied the inhibitor activity site after the coordination of the inhibitor and copper, which led decreased quenching of tyrosinase.

3.3. ^{1}H NMR and ^{13}C NMR titration studies

To investigate the bonding mode between the inhibitor and tyrosinase, we used ^{1}H NMR and ^{13}C NMR titrations to identify the bonding mode between different molecules by determining the chemical shifts of hydrogen and carbon atoms [41]. The interactions between compounds **1**, **6**, **8** and tyrosinase were further observed from ^{1}H NMR titrations in DMSO-d6. The titrations were carried out by addition of tyrosinase to inhibitor in different concentrations and their NMR plots were collected (Fig. 5). Upon the addition of 0.341 mg/mL (Final concentration) of tyrosinase to the target compounds **1** or **6** or **8**, in Fig. 5(A), the peaks at 11.45/11.45/11.47 ppm (of –CSNH–, Ha) almost completely disappeared. This was caused by the tautomeric effect, in which NH-C=S was transformed into N=C-SH. Then, the sulfur atom donated hydrogen and formed a complex with enzymic Cu^{2+} and led to the disappearance of the -CSNH- proton. The peaks at 8.22/8.23/8.23ppm(amino proton, $–NH_2$, Hb) gradually shifted to 8.14 / 8.12 / 8.13ppm with the dropwise addition of the enzyme,

which indicated that the increase of the electron density on amino proton due to formation of hydrogen bond between -NH_2 group proton and tyrosinase. The result was consistent with molecular docking for compound **8**, the Hb form hydrogen bonds with GLU265. The peaks at 7.59/7.59 ppm (-CH=N-, Hc) for compounds **1** and **6** moved to 7.62/7.61ppm with the addition of enzyme solution, which suggested that the original system (-CH=N-) translated the new big conjugate system (-CH=N-N=C-) causing the electron cloud density of Hc is reduced, and the chemical shift value δ of Hc is enhanced. The peak at 7.54 ppm (He, benzene-H) for the compound **8** split into two peaks (7.58 ppm and 7.53 ppm) with the addition of enzyme solution. It suggests that there exist some interactions between benzene-H atom of benzene ring and enzyme changing the electric density and chemical micro-environment of benzene-H atom differently. The results were well explained by assuming that there existed an inter-molecular interaction besides formation of hydrogen bond and complexes between the compound **8** and tyrosinase in the latter research of molecular docking studies.

The interactions between compound **8** and tyrosinase were further observed from the ^{13}C NMR titrations in DMSO-d6 (Fig.5B). Upon the addition of 0.406 mg/mL of tyrosinase to compound **8**, the chemical shift values of C1(-C=S , 177.389ppm) and C3 (-C=N-, 139.126ppm) moved upfield (177.011, 138.747 ppm), while C4 (2 -thiophene) moved downfield from137.212 to 137.484 ppm, which indicated that the electron density increased in the carbon atoms on -C=S and -C=N- group and decreased in the carbon atoms on 2-thiophene.This occurred due to existing of big

conjugated system(thiophene-C=N-N=C-S-). Moreover, the chemical shift value of C2(-C=O) of 4-functionalized ester group moved downfield from165.354 to 165.422 ppm, which may root from the formation of hydrogen bond between the oxygen atom on C2 and amino acid residues of HIS85(molecular docking shown in Fig. 6A). The chemical shift values of C5 (benzene ring) moved upfield from 129.887 to 128.944 ppm. This suggested that there existed an interaction between benzene ring group and enzyme, which was in good conformity with results of the above ^{1}H NMR titration and well explained by the subsequent molecular docking studies.

3.4. Molecular docking study

The configuration of the binding complexes of tyrosinase with compound **8** by using Accelry Discovery studio 2.0 was shown in Fig. 6. The relevant parameters of molecular docking were -26.9452 kcal mol^{-1} (CDDOCKR-ENERGY) and -31.8851 kcal mol^{-1} (CDDOCKR-INTERACTION-ENERGY). From Fig. 6A , it was indicated that amino acid residues of ASN206, GLU256, HIS85 may form hydrogen bonds with -NH-, -NH_2 and -C=O of compound **8** molecules, respectively. Obviously the formation of these hydrogen bonds may greatly promote the formation of complexes between inhibitor and tyrosinase and enhance the inhibitory activity of the tested compound accordingly. Interestingly, it was observed that there was an additional inter-molecular interaction shown in Fig. 6B between benzene ring group from inhibitor and amino acid residues ASN81 from enzyme, which may lead the electronic density and chemical micro-environment of hydrogen atoms of benzene ring to change differently and split NMR peaks of hydrogen atoms of benzene ring into

multiple peaks. The result was well coincident with the observed multiple peak (He, benzene-H) finding of NMR titration. It was postulated that the inter-molecular interaction (Van der Waals force including interactions of electrostatic, polarity and dispersion) existing in inhibitor and hydrophobic domain of enzyme active center may help to stabilize the complexes formed between inhibitor and enzyme, which surely further promotes and enhances the inhibitory activity of the tested compound in addition to the promoting effect of complexes formation. The amino residues of HIS269, HIS244, ASN81 (the purple circles of 2D at Fig. 6A） may involve in the interaction of electrostatic or polarity between inhibitor and enzyme, whereas the HIS263, PHE90, VAL283 (the green circles of 2D at Fig. 6A） of enzyme involve in interaction of dispersion with the benzene ring moiety of the compound **8** (explanation of Fig. 6A can be found in Tutorials of Discovery studio 2.0)**.** The promoting effect from inter-molecular interaction was verified by the spectrofluorimetry studies.

4. Conclusion

Novel Tyrosinase inhibitors of 4-functionalized TCT derivatives (**1**-**8**) had been synthesized and spectrofluorimetry, 1H and 13C NMR titration and molecular docking had been used to investigate their inhibitory activities and mechanisms on tyrosinase. We found that there existed an additional inter-molecular interaction between benzene ring of compound **8** and amino acid residue of ASN81 in hydrophobic domain of enzyme active center besides common formation of hydrogen bonds and auxiliary vicinity synergistic effect, which helps to further stabilize the

complexes formation between the sulfur atom of the thiourea group in the inhibitor and the dicopper ions of the enzyme active center and surely promotes the inhibitory activity of the compound **8**. All of these effects led a 68.52% enhancement of inhibitory activity of compound **8** (IC_{50} =0.068 μM) compared to that of its analog of 4-acetyl methoxy-TCT (compound **2**). The finding was well explained by molecular docking studies, verified by and consistent with experiments of spectrofluorimetry, ^{1}H and ^{13}C NMR titration. The 4-benzoy methoxy substitution of the TCT successfully produced novel inhibitors of tyrosinase in mushroom. Additional research including toxicity is necessary to develop novel and highly potent tyrosinase inhibitors.

Acknowledgments

This work was supported by National Natural Sciences Foundation of China (No. 20962014) and the free searching foundation of State Key Laboratory of Food Science and Technology (Nanchang University) in China (SKLF-TS-200914).

References

[1]P. Ruzza, P. A. Serra, D. Fabbri, M. A. Dettori, G. Rocchitta, & G. Delogu. Hydroxylated biphenyls as tyrosinase inhibitor: A spectrophotometric and electrochemical study. Eur. J. Med. Chem, 126 (2016), 1034-1038.

[2]Y. Motabo, T. Kumagai, A. Yamamoto, H Yoshitsu, & M. Sugiyama. Crystallographic Evidence That the Dinuclear Copper Center of Tyrosinase Is Flexible during Catalysis. J. Biol. Chem, 281 (2006), 8981–8990.

[3] A. M. Mayer. Polyphenol Oxidases in Plants and Fungi: Going Places?A review. Phytochem, 67(2006), 2318-2331.

[4] B. M. Christensen, J. Li, C. C. Chen, A.J. Nappi, Melanization immune responses in mosquito vectors. Trends Parasitol, 21(2005), 192–199.

[5] S. J. Yin, K. J. Liu, J. Lee, J. M. Yang, G. Y. Qian, Y. X. Si, & Y. D. Park.Effect of Hydroxysafflor Yellow A on Tyrosinase: Integration ofinhibition kinetics with computational simulation. Process Biochem, 50(2015), 2112-2120.

[6] J. Choi, S. J. Park, & J. G. Jee.Analogues of ethiona mide, a drug used for multidrug-resistant tuberculosis, exhibit potent inhibition of tyrosinase. Eur. J. Med. Chem, 106(2015), 157–166.

[7] T. Pan, X. Li, & J. Jankovic.The association between Parkinson's disease and melanoma. Int. J. Cancer, 128 (2011), 2251–2260.

[8] M. Friedman, Chemistry, biochemistry, and dietary role of potato polyphenols.A review. J. Agric. Food. Chem, 45(1997), 1523-1540.

[9] K. U. Zaidi, A. S. Ali, S .A. Ali. I. Naaz. Microbial Tyrosinases: Promising Enzymes for Pharmaceutical, Food Bioprocessing, and Environmental Industry.Biochem Res Int, 2(2014), 854-687.

[10] A. Garcia-Jimenez, J. A. Teruel-Puche, J. Berna, J. N. Rodriguez-Lopez, J. Tudela, P. A. Garcia-Ruiz.Characterization of the action of tyrosinase on resorcinols. Bioorg.Med. Chem, 24(2016), 4434-4443.

[11] S. Ferro, L. D. Luca, M. P. Germanò, M. R. Buemi, L. Ielo, G. Certo. Chemical exploration of 4-(4-fluorobenzyl) piperidine fragment for the development of new tyrosinase inhibitors.Eur.J.Med. Chem, 125(2017), 992–1001.

[12] M. Verdoni, H. Roudaut, H. D. Pomyers, D. Gigmesa, D. Bertina, J. Luisc& K. Mabrouk. ArgTX-636, a Polyamine isolated from spider venom: A novel class of melanogenesis

inhibitors.Bioorg. Med. Chem, 24(2016), 5685–5692.

[13]S. Briganti, E. Camera, M. Picardo.Chemical and Instrumental Approaches to Treat Hyperpigmentation.Pigment cell & melanoma research, 16(2003), 101-110.

[14] J. Xie, H. H. Dong, Y. Y. Yu. & S. W. Cao, Inhibitory effect of synthetic aromatic heterocycle thiosemicarbazone derivatives on mushroom tyrosinase: Insights from fluorescence, 1H NMR titration and molecular docking studies. Food Chem, 190(2016), 709–716.

[15]J. Xu, J. Liu, X.Q. Zhu, Y. Y. Yu, & S.W. Cao. Novel inhibitors of tyrosinase produced by the 4-substitution of TCT.Food Chem, 221(2017), 1530-1538.

[16] Y. L. Gol'dfarb, A. P. Yakubov, L. I. Belen'Kii.Reactions of aromatic and hetero aromatic compounds containing electron-acceptor substituents. Chem. Heterocycl. Compd, 14(1986), 1196-1198.

[17] V. Ryabova, L. Ignatovich.Thiophene Substitution Chemistry.Springer International Publishing, 39(2014), 43-108.

[18] H. Z. Song, S. M. Ding,A Convenient Method for Preparing 3-Hydroxymethylthiophene.Mod Chem Ind, 24(2004), 38.

[19] G. Q. Lai, Q. Fang, X. L. Ren, Y. J. Shen.Hydrolysis of 4, 4’-bis (chloromethyl) biphenyl in acetonitrile / water. Chin. J. Chem. Eng, 20 (2006), 1013-1016.

[20] D. Wu, W. Wen, S. Chen, H. Zhang. Preparation and properties of a novel form-stable phase change material based on a gelator. J. Mater.Chem. A, 3(2015), 2589-2600.

[21] Q. X. Chen.Enzymology and Research Techonlogy, chapter 5.Xiamen University Press. Xiamen, 2010, pp. 118-119.

[22]Y. J. Wang, G. W. Zhang, J. K. Yan, & D. M. Gong. Inhibitory effect of morin on tyrosinase: Insights from spectroscopic and molecular docking studies. Food Chem, 163(2014), 226–233.

[23] A. S. Karikari, B. D. M.And, T. E. Long.Association of Star-Shaped Poly (D, L-lactide) s Containing Nucleobase Multiple Hydrogen Bonding.Biomacromolecules, 8(2007), 302-8.

[24] Z. Li, G. W. Zhang, S. Lin, D. M. Gong.Inhibitory Mechanism of Apigenin on α-Glucosidase and Synergy Analysis of Flavonoids. J. Agric. Food. Chem, 123(2016), 6–13.

[25] N. Shahabadi, M. Maghsudi, & S. Rouhani, Study on the interaction of food colourant quinoline yellow with bovine serum albumin by spectroscopic techniques. Food Chem, 135(2012), 1836–1841.

[26] K. Ghosh, S. Rathi, D. Arora, Fluorescence spectral studies on interaction of fluorescent probes with Bovine Serum Albumin (BSA).J. Lumin, 175(2016), 135–140.

[27] X. Fradera, R. M. Knegtel, J. Mestres.Similarity-driven flexible ligand docking.Proteins Struct. Funct.Bioinf, 40(2000), 623–636.

[28] B. Gopalakrishnan, V. Aparna, J. Jeevan, M. Ravi, G. R. Desiraju.A virtual screening approach for thymidine monophosphate kinase inhibitors as antitubercular agents based on docking and pharmacophore models. J. Chem. Inf. Model, 45(2005), 1101–1108.

[29]E. Perola, Minimizing false positives in kinase virtual screens.Proteins Struct. Funct.Bioinf, 64(2006), 422–435.

[30] Q. Y. Xing, W. W. Pei.Basic Organic Chemistry (3rd edition), chapter 6.Higher Education Press, Beijing, 2005, pp.243-246.

[31] Y. Cui, G Liang, Y. H Hu, Y. Shi, Y. X. Cai, H. J. Gao, Q. X. Chen, and Q. Wang. Alpha-substituted derivatives of cinnamaldehyde as tyrosinase inhibitors: inhibitory mechanism and molecular analysis. J. Agric. Food. Chem, 63(2015), 716-722.

[32] J. Y. Wang, S. G. Zhu, C. F. Xu.Biochemistry (3rd edition), chapter 9.Higher Education Press.Beijing, 2002, pp.369-370.

[33] D. Li, T. Zhang, C. Xu, B. Ji.Effect of pH on the interaction of baicalein with lysozyme by spectroscopic approaches. J. Photochem. Photobiol.B, 104(2011), 414–424.

[34] Y. Q. Wang, B. P. Tang, H. M. Zhang, Q. h. Zhou, G. C. Zhang. Studies on the interaction between imidacloprid and human serum albumin: spectroscopic approach. J. Photochem. Photobiol.B, 94(2009), 183-190.

[35] S. R. Feroz, S. B. Mohamad, N. Bujang, S. N. Malek, S. Tayyab.Multispectroscopic and Molecular Modeling Approach To Investigate the Interaction of Flavokawain B with Human Serum Albumin.J. Agric.Food.Chem, 60 (2012), 5899-5908.

[36] M. S. Zaroog, S. Tayyab. Formation of melting globule-like state during acid denaturation of Aspergillus niger, glucoamylase. Process Biochem, 47(2012), 775-784.

[37] J. K. Yan, G. W. Zhang, Y. T. Hu, Y. D. Ma. Effect of luteolin on xanthine oxidase: Inhibition kinetics and interaction mechanism merging with docking simulation. Food Chem, 141(2013), 3766-3773.

[38] Z. J. Cheng, Studies on the interaction between scopoletin and two serum albumins by spectroscopic methods. J. Lumin, 132(2012), 2719–2729.

[39]J. R. Lakowicz, Principles of Fluorescence Spectroscopy, Springer Publications, New York, 2006.

[40] I. J. Joye, G. Davidov-Pardo, R. D. Ludescher, & D. J. McClements, Fluorescence quenching study of resveratrol binding to zein and gliadin: Towards a more rational approach to resveratrol encapsulation using waterinsoluble proteins. Food Chem, 185(2015), 261–267.

[41] J. O. Park, S. K. Sahoo, & H. J. Choi.Design, synthesis and 1H NMR study of C3v-symmetric anion receptors with urethane-NH as recognition group. Spectrochim.Acta, Part A, 153(2016), 199–205.

Fig.1. Synthesis of 4-functionalized thiophene-2-carbaldehyde thiosemicarbazone derivatives **1**-**8**

.

Fig.2.(A) Effect of concentrations of mushroom tyrosinase on its activity for the oxidation of L-DOPA at different concentrations of compound **1**, **3**-**8**. Concentrations of compounds for cures 0-3 were 0, 0.04, 0.16, 0.64 μM, respectively. (B) Relative enzymatic activity of compounds **1**-**8**. (C) Lineweaver-Burk plots of mushroom tyrosinase on the presence of compound **1**, **3**-**8** during the oxidation of L-DOPA. Concentrations of compounds for curves 0-3 were 0, 0.04, 0.16 and 0.64 μM.

Fig.3. Synchronous fluorescence spectra of tyrosinase in the absence and presence of compound **6**: (A) $\Delta\lambda$ = 15 nm or (B) $\Delta\lambda$ = 60 nm (pH 6.8, T = 298 K). c (tyrosinase) = 30 μg/ mL. c (compound 6) =0, 11.97, 23.88, 35.73, 47.52, 59.26 and 70.94 μM, respectively. Three-dimensional fluorescence spectra of tyrosinase (a), the compound **1**+tyrosinase system (b), the compound **6**+tyrosinase system (c) and the compound **8**+tyrosinase system (d), which the concentrations of compounds of system were 35.73 μM.

Fig.4. Fluorescence spectra of tyrosinase in the absence and presence compound **6** or **6**-Cu^{2+} complex: (A) compound **6; (B)** compound **6**-Cu^{2+}complex.Concentrations for curves were 0, 5.99, 11.94, 17.87, 23.76, 29.63, 35.47, 41.28, and 47.06 μM, respectively. The inset of (A) depicts Stern–Volmer plots for the fluorescence quenching of tyrosinase by compound **6** at 30, 35 and 40 °C. The inset of (B) depicts Stern–Volmer plots for the fluorescence quenching of tyrosinase by compound **6**-Cu^{2+}complex at 30 °C.

Fig.5. (A) ^{1}H NMR titration studies of compounds **1**, **6**, **8** (21 mM) with tyrosinase in DMSO-d6 solvent.The concentrations of tyrosinase ranging from 0, 0.098 to 0.341 mg/mL. (B) ^{13}C NMR titration of compound **8** (62.6 mM) in DMSO-d6 was prepared and titrated with tyrosinase from 0 to 0.406 mg/mL.

Fig.6. Molecular docking of compound 8 with tyrosinase. (A) 2D structure for the interaction of compound **8** with tyrosinase.Purple circles represent the amino acids which involved in the formation of hydrogen bonding, interaction of lectrostatic or polarity, green circle represent in van der Waals interaction of amino acids, The dotted line represents a hydrogen bond, the arrow pointing in the direction of electron donor. Shadows represent close contacts. (B) Corresponding tertiary structures of tyrosinase residues interact with compound 8. The dotted yellow line stands for hydrogen bonds or close contacts.

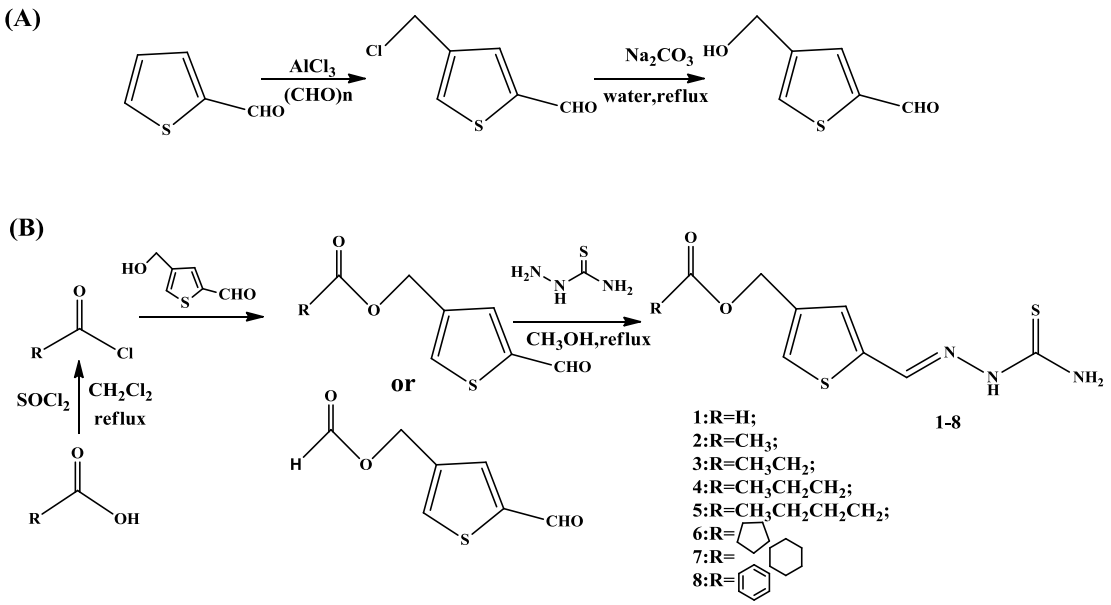

International Journal of Biological Macromolecules, Jing Liu[a], Mengrong Li[a], Yanying Yu [a], Shuwen Cao [a,b]*, **Fig. 1.**

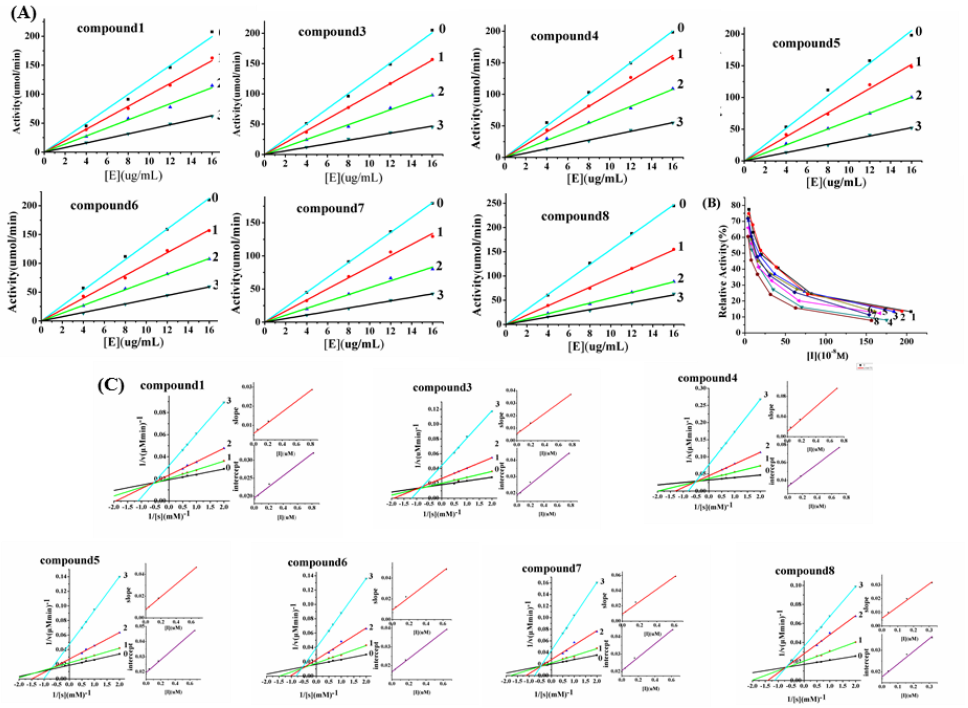

International Journal of Biological Macromolecules, Jing Liu[a], Mengrong Li[a], Yanying Yu [a], Shuwen Cao [a,b]*, **Fig. 2.**

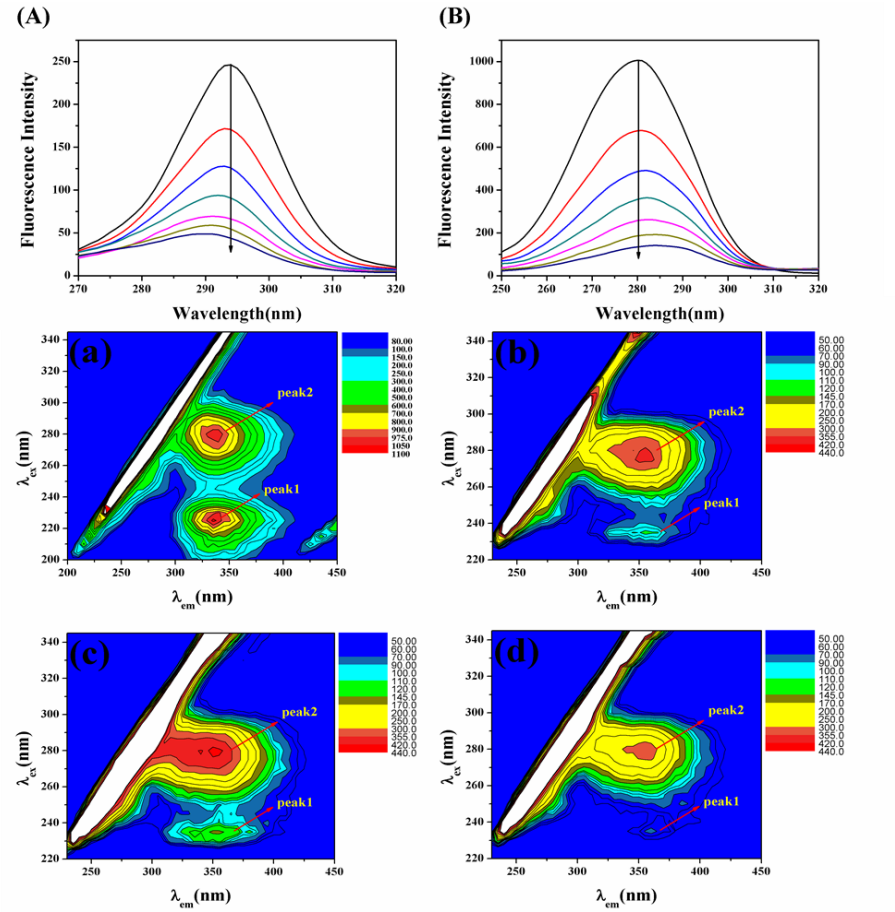

International Journal of Biological Macromolecules, Jing Liu[a], Mengrong Li[a], Yanying Yu [a], Shuwen Cao [a,b]*, **Fig. 3.**

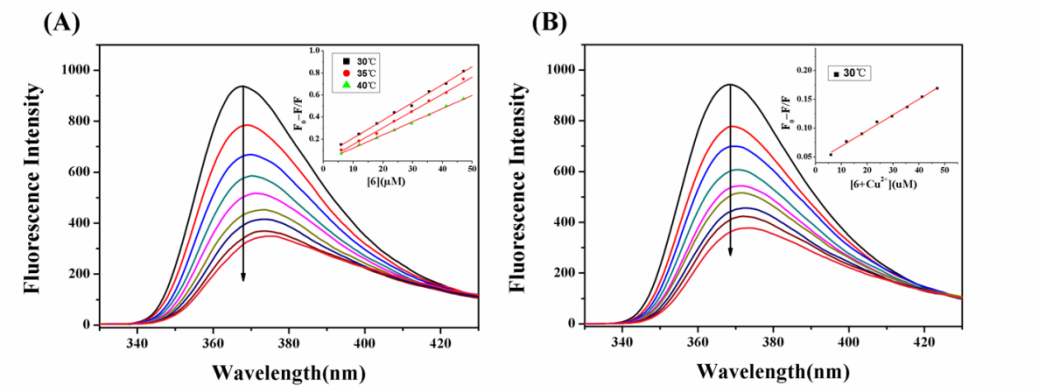

International Journal of Biological Macromolecules, Jing Liu[a], Mengrong Li[a], Yanying Yu [a], Shuwen Cao [a,b]*, **Fig. 4.**

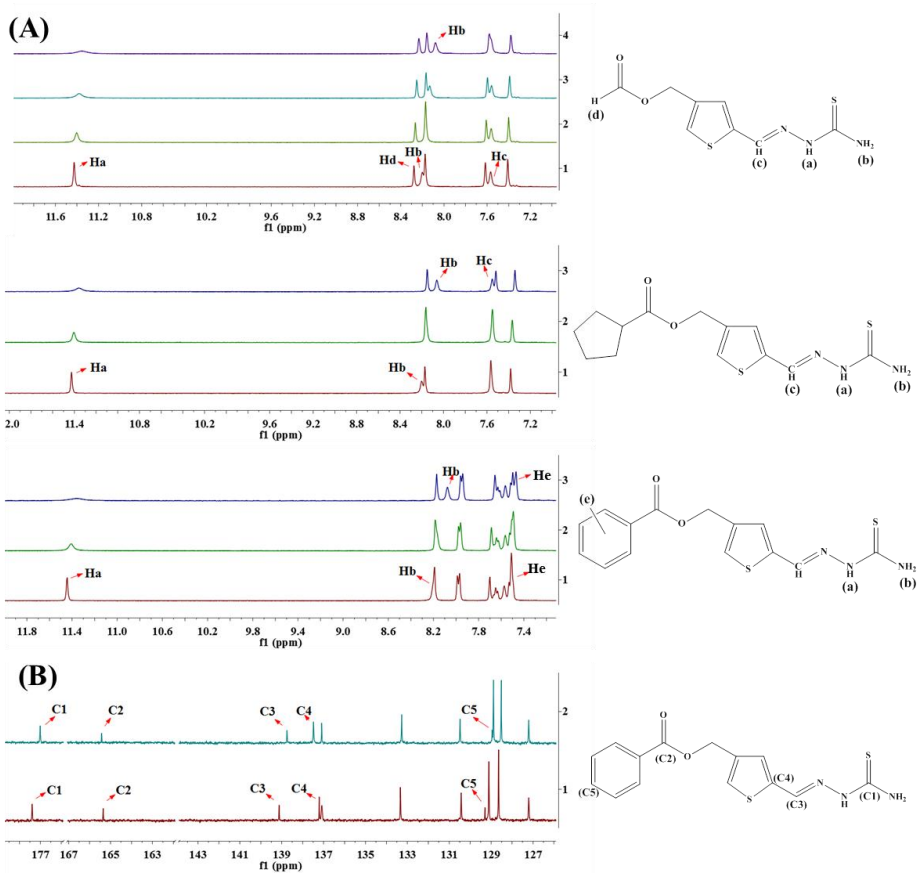

International Journal of Biological Macromolecules, Jing Liu[a], Mengrong Li[a], Yanying Yu [a], Shuwen Cao [a,b]*, **Fig. 5.**

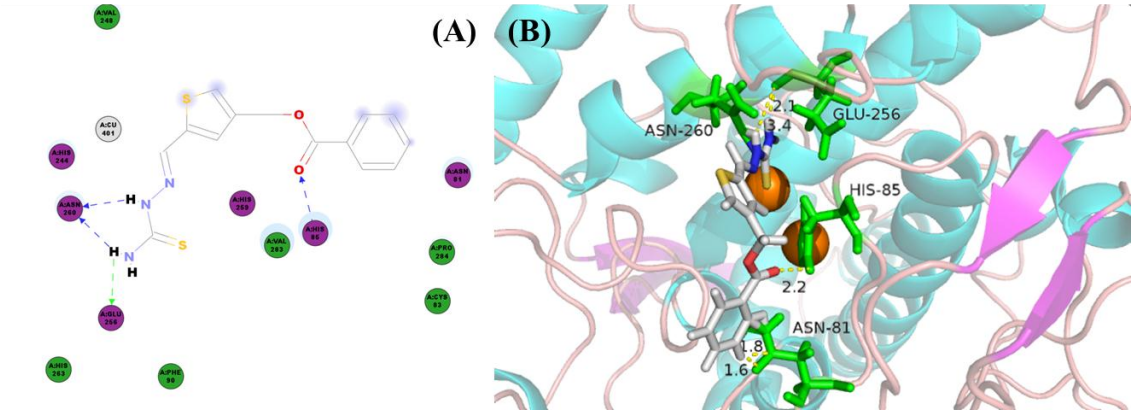

International Journal of Biological Macromolecules, Jing Liu[a], Mengrong Li[a], Yanying Yu [a], Shuwen Cao [a,b]*, **Fig. 6.**

Table 1

Structure, Inhibitory activity of compounds **1**-**8** on mushroom tyrosinase;The Stern-Volmer quenching constants K_{SV}, the quenching rate constants K_q and the binding constant K_a.

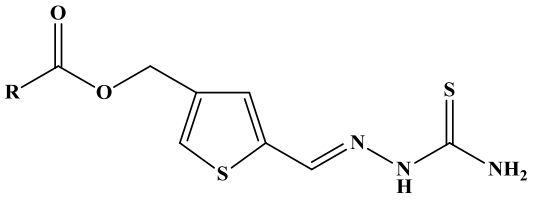

		1	2*	3	4	5	6	7	8	6-Cu^{+2}	TCT	Kojic acid
R		H	CH_3	CH_3CH_2	$CH_3(CH_2)_2$	$CH_3(CH_2)_3$						
IC_{50} (μM)		0.196	0.216	0.161	0.105	0.110	0.140	0.136	0.068		0.43	19.68
K_I(μM)		0.78	0.33	1.74	1.89	2.13	2.12	1.86	3.31			-
K_{IS}(μM)		4.79	0.7	7.11	11.16	7.36	6.67	8.48	14.42			-
K_{SV}(10^4L·mol^{-1})	30°C	0.968	1.081	1.038	1.328	1.244	1.249	1.337	1.532	0.462		-
	35°C	0.766					1.299		1.301			-
	40°C	1.102					1.113		1.176			-
K_q(10^{12}L·mol^{-1}·s^{-1})	30°C	0.968	1.081	1.038	1.328	1.244	1.249	1.337	1.532	0.462		-
	35°C	0.766					1.299		1.301			-
	40°C	1.102					1.113		1.176			-
lgK_a(L·mol^{-1}·s^{-1})	30°C	3.814	4.101	4.051	4.057	3.910	4.022	4.079	4.725	2.255		-
	35°C	3.792					3.903		4.091			-
	40°C	3.851					3.877		4.038			-

2* synthesized and reported by our laboratory before.

Table 2

Parameters of the 3D fluorescence for compound **1-8** with tyrosinase binding.The Concentrations of compounds of system were 0 and 35.73 μM.

Compound	1		2		3		4		5		6		7		8	
Peak	**Peak1**	**Peak2**	**Peak1**	**Peak2**	**Peak1**	**Peak2**	**Peak1**	**Peak2**	**Peak1**	**Peak2**	**Peak1**	**Peak2**	**Peak1**	**Peak2**	**Peak1**	**Peak2**
Start position ($\lambda_{ex}/\lambda_{em}$) (nm)	225.0/ 335.0	280.0/ 335.0	225.0/ 340.0	280.0/ 335.0	225.0/ 335.0	280.0/ 330.0	225.0/ 330.0	280.0/ 330.0	225.0/ 330.0	280.0/ 335.0	225.0/ 345.0	280.0/ 335.0	225.0/ 340.0	280.0/ 335.0	225.0/ 335.0	280.0/ 330.0
Last position ($\lambda_{ex}/\lambda_{em}$) (nm)	235.0/ 360.0	280.0/ 350.0	235.0/ 360.0	280.0/ 360.0	235.0/ 360.0	280.0/ 365.0	235.0/ 360.0	280.0/ 360.0	235.0/ 355.0	280.0/ 360.0	235.0/ 370.0	280.0/ 360.0	235.0/ 375.0	280.0/ 360.0	235.0/ 370.0	280/ 350.0
Start relative intensity (IF)	947.7	682.3	788.2	606.5	817.1	656.3	884.7	623.9	805.4	623.2	806.6	607.3	681.4	541.3	852.4	632.8
Last relative intensity (IF)	100.7	266	82.19	212	86.79	214.5	94.33	204.2	100	215.4	114.8	227.8	116.2	225.1	78.57	251.3
$(F_0\text{-}F/F_0)\%$	89.37	61.01	89.57	65.05	89.38	67.32	89.34	67.27	87.58	65.44	85.77	62.49	82.95	58.41	90.78	60.29
$\Delta\lambda_{ex}/\Delta\lambda_{em}$ (nm)	10/25	0/15	10/20	0/25	10/25	0/35	10/30	0/30	10/15	0/25	10/25	0/25	10/35	0/25	10/35	0/20